Reclassification of epithelial ovarian tumors by comparative proteomics

Yong Kyu Park

Department of Medicine

The Graduate School, Yonsei University

Reclassification of epithelial ovarian tumors by comparative proteomics

Yong Kyu Park

Department of Medicine

The Graduate School, Yonsei University

Reclassification of epithelial ovarian tumors by comparative proteomics

Directed by Professor Sei Kwang Kim

The Doctoral Dissertation
submitted to the Department of Medicine,
the Graduate School of Yonsei University
in partial fulfillment of the requirements for the
degree of Doctor of Philosophy

Yong Kyu Park

December 2005

This certifies that the Doctoral Dissertation of Yong Kyu Park is approved.

Thesis Supervisor : Sei Kwang Kim

Nam Hoon Cho: Thesis Committee Member#1

Young Tae Kim: Thesis Committee Member#2

Hyeyoung Kim: Thesis Committee Member#3

Sun Young Rha: Thesis Committee Member#4

The Graduate School
Yonsei University

December 2005

ACKNOWLEDGEMENTS

본 논문이 완성되기까지 세심한 지도와 무한한 사랑과 관심으로 이끌어 주신 김세광 교수님께 진심으로 감사 드리며 많이 부족한 저에게 항상 너그럽고 자상하게 지도해 주시고 격려해 주신 조남훈 교수님께도 깊은 감사 드립니다.

아울러 논문 완성에 세심한 지도 편달과 관심을 아끼지 않으신 김영태 교수님, 김혜영 교수님과 라선영 교수님께도 깊은 감사를 드립니다.

오늘이 있기까지 사랑과 격려로 이끌어 주신 부모님과 사랑하는 아내 상희와 아들 준우에게 이 논문을 바칩니다.

저자 씀

TABLE OF CONTENTS

LIST OF FIGURES

LIST OF TABLE

Abstract

Reclassification of epithelial ovarian tumors by comparative proteomics

Yong Kyu Park

Department of Medicine

The Graduate School, Yonsei University

(Directed by Professor Sei Kwang Kim)

We analyzed twelve epithelial ovarian tumors using proteomics to construct intra- and inter-tumoral distance map trees. The following tumors were used: 4 serous tumors including 1 low malignant potential (LMP) tumor and 3 serous carcinomas, 5 mucinous tumors including 2 LMP tumors, 2 LMP tumors with aggressive features, and 1 widely invasive mucinous carcinoma, and 3 endometrioid tumors including 1 endometriotic cyst and 2 carcinomas. Proteins extracted from frozen slides microdissected by laser capture microdissector (LCM) were prepared for 2D-E gel, where only the spots that clearly showed a greater than a two-fold change in expression compared to controls were selected.

We performed protein profile distance comparison and clustering analysis. Epithelial ovarian tumors and normal tissues showed an apparent separation on the distance map tree. Mucinous carcinomas were nearest to the normal group, whereas serous carcinomas were the greatest distance from the normal group. All mucinous tumors with aggressive histology were separated from the LMP group.

The benign-looking cysts adjacent to the IEC (intraepithelial carcinoma) showed an expression pattern identical to the IEC area. The extent of change on the lineages leading to the mucinous and serous carcinoma was 1.98-fold different. The overall gene expression profiles of serous or endometrioid carcinomas appeared to be less affected by grading or stage than by histologic type.

In conclusion, ovarian mucinous tumors are apparently distinct from other epithelial ovarian tumors. The LMP mucinous tumors showing histologic aggressive features belong to mucinous carcinoma on the molecular basis. The morphologic continuous spectrum in mucinous carcinoma has the same gene expression profiles.

Key Words : epithelial ovarian tumor, proteomics, distance map tree, low malignant potential

Reclassification of epithelial ovarian tumors by comparative proteomics

Yong Kyu Park

Department of Medicine

The Graduate School, Yonsei University

(Directed by Professor Sei Kwang Kim)

I. INTRODUCTION

Despite the critical importance of understanding epithelial ovarian tumors, carcinogenesis in epithelial ovarian cells is the least understood in cancer research. The majority of epithelial ovarian tumors are believed to be derived from the ovarian surface epithelium (OSE).[1,2,3] Epithelial ovarian tumors have a unique spectrum consisting of benign cystadenoma, low malignant potential (LMP) epithelial tumors, and frankly invasive carcinoma.[4,5]

LMP tumors are intermediary between those of clearly benign and clearly malignant tumors of the same cell type in both histopathological and biological aspects. However, the characterization of LMP tumors has been controversial for more than a century.

Furthermore, LMP tumors occasionally manifest as bothersome clinical presentation, such as peritoneal implants in serous tumors and pseudomyxoma peritonei in mucinous tumors.[6]

Most ovarian carcinomas seem to arise de novo from OSE. However, approximately 5-10% of carcinomas may arise in a stepwise manner from borderline tumors.[5,7] More specifically, many mucinous carcinomas often exhibit a wide spectrum, ranging from benign to malignant epithelium in the same tumor. Moreover, there is focal abrupt transition from benign to borderline or malignant epithelium.[8] Recently, a continuous pathological spectrum based on multistep carcinogenesis has been accepted in some well-differentiated mucinous tumors, including benign mucinous cystadenoma, LMP mucinous tumor, intraepithelial carcinoma (IEC), stromal microinvasion and widely invasive mucinous carcinoma.[6,8]

According to most studies that have attempted to define the validity of this spectrum in the biological aspect, IEC with stromal microinvasion, by definition having more than one isolated microinvasive focus of stromal invasion measuring less than 10 mm^2 in area, is regarded as a category of LMP, because of its favorable outcome.

However, there has not yet been any verification of the spectrums of IEC or microinvasion, and whether it is similar to LMP in the molecular aspects. Moreover, the follow-up periods of previous studies have been too short to determine the clinical relevance of tumors showing histologic aggressive features in the LMP category. Nonetheless, there have been rare molecular studies to compare between

ovarian tumors of LMP and those with aggressive features.

Morphological heterogeneity and difficulties in discrimination upon gross examination are the main causative factors of the extreme rarity of molecular studies of ovarian tumors. Furthermore, insufficiency and easy degeneration of proteins, when they were extracted from multilocular cysts of mucinous tumors, make it difficult to rely on literature regarding the molecular properties. Accordingly, studies using proteomics or cDNA arrays with tissues from patients have rarely been performed, likely due to those limitations,[9,10] while studies using serum of patients may have ever been performed.[11,12]

The proteomics analysis of protein expression patterns in OSE-derived tumors can provide new insight into dysregulated cell signaling pathways, which may in turn lead to the development of promising treatments.[10,13] In the present proteomics study, a distance tree based on intra- and inter-tumoral variations of gene expression patterns enabled us to determine similarities between several organs from different species of primates.[14] Differences in apparent protein expression levels were used to calculate an overall map distance summarized over all genes.[15]

In this study, we aimed to reclassify ovarian epithelial tumors with different histological types and grades and to determine the proteomic similarities or differences between conventional LMP tumors and LMP tumors with histologic aggressive features, such as IEC or microinvasion using a distance map tree.

II. MATERIALS AND METHODS

1. Tissue preparation and laser capture microdissection

All tumors and corresponding normal tissues were stored in sterile bottles in a deep freezer. Prior to protein extraction, all cases were examined on cryosections, and again matched with the paraffin-embedded tissues. A total of 12 epithelial ovarian tumors: 4 serous tumors including 1 LMP tumor and 3 serous carcinomas; 5 mucinous tumors, including 2 LMP tumors and 2 LMP tumors with aggressive features (1 intraepithelial carcinoma and 1 with stromal microinvasion), and 1 widely invasive mucinous carcinoma; 3 endometrioid tumors, including 1 endometriotic cyst and 2 carcinomas, were analyzed using proteomics.

Frozen slides were prepared from each case and microdissected by LCM with a Zeiss Axiovert 135 System (Zeiss, Oberkochen, Germany). Frozen tissue specimens were cut into a series of 6mm-thick sections and mounted on slides coated with a thermoplastic membrane (PEN foil slides; Leica Microsystems, Wetzlar, Germany). Cystic tumor cells were selectively dissected by focal melting of the membrane with a UV-laser beam (337 nm) set to pulse at 80 kW. Microdissected fragments were dropped into cap-tubes under microscope inspection. To minimize degradation, slides were fixed with 70% ethanol for 1 min, washed in diethylpyrocarbonate (DEPC)-treated deionized water, and stained with a Histogene LCM kit (Arcturus, Mountain View, CA, USA) to preserve the integrity of cellular nucleic acids. Based on careful review of the histologic sections, each microdissection was

estimated to contain >98% of the desired cells. Areas with luminal secretion, bloody substance, and necroinflammation were avoided.

2. Protein extraction and 2-D gel electrophoresis

Tissue samples from patients were washed with PBS/phosphate inhibitor, incubated in lysis buffer [40 mM Tris-HCl, 7 M urea, 2 M thiourea, 4% 3-[(3-cholamidopropy) dimethyammonio]-1-propanesulfonate (CHAPS; Sigma-Aldrich, St. Louis, MO, USA), 100 mM 1, 4-dithioerythtitol (DTT; Sigma-Aldrich, St. Louis, MO, USA) with a protease inhibitor cocktail (Sigma-Aldrich, St. Louis, MO, USA)], and the samples were shaken for 15 minutes. Subsequently, lysates were incubated at 4°C for 40 minutes with vigorous shaking every 10 minutes, and then centrifuged at 4°C for 30 minutes at 14,000 rpm. The protein-containing supernatant was transferred to a new tube, and then the protein concentration determined using a Bio-Rad Protein Assay (Bio-Rad, Hercules, CA, USA).

Nonlinear gradient strips, pH 4–10 were equilibrated by applying 7 M urea containing 2% CHAPS, 1% DTT, 1% pharmalyte, and 2 M thiourea for 12–16 hours; 200 μg of sample was loaded onto each strip. Isoelectric focusing (IEF) was performed using a Multiphor II electrophoresis unit and an EPS 3500 XL power supply (Amersham Biosciences, Uppsala, Sweden) at 20°C. During IEF, the voltage was slowly increased over 3 hours from 150 V to 3,500 V. Prior to the second dimension, the strips were incubated in equilibration buffer [6 M urea, 2% SDS, 50 mM Tris-HCl, pH 6.8, and 30 % glycerol] for 10 minutes. At that time, 1% DTT was added the first time, and

subsequently 2.5% iodoacetamide (Sigma-Aldrich, St. Louis, MO, USA) was added. The equilibrated strips were inserted into SDS-PAGE gels (20-24cm, 10−16%), and SDS-PAGE was performed using a Hoefer DALT 2D system (Amersham Biosciences, Uppsala, Sweden). 2D gels were downloaded at 1,700 Vh at 20°C and treated with silver staining

3. Image analysis

An image analysis was performed using a PDQuest software (version 7.0; Bio-Rad, Hercules, California, USA), and the amount of protein in each spot was normalized to the total valid spot intensity. Only the spots that clearly showed a greater than a two-fold change in expression compared to controls were selected.

4. MALDI-TOF-MS

For each gel spot, a biopsy punch was prepared and transferred to a 1.5 mL siliconized Eppendorf tube (Ambion, Austin, TX, USA). Subsequently, the transferred gel-spots were destained in destaining solution [100 mM $Na_2S_2O_3$ (Sigma-Aldrich, St. Louis, MO, USA) and 30 mM $K_3Fe(CN)_6$ (Sigma-Aldrich, St. Louis, MO, USA)(V/V, 1:1)]. The destained gel slices underwent pre-reduction using 100% acetonitrile (HPLC grade). Gel-spots containing protein were reduced at 56°C for 30 minutes in reduction buffer [100 mM NH_4HCO_3 (Sigma-Aldrich, St. Louis, MO, USA), 10 mM DTT (Sigma-Aldrich, St. Louis, MO, USA)], and alkylated at room temperature for 25 minutes in alkylation buffer [100 mM NH_4HCO_3 and 55 mM iodoacetamide]. Gel slices were dried in a Speed-Vac (GMI, Ramsey, MN, USA).

The dried gel slices were incubated at 37°C for 12–16 hours in ABC buffer [50mM ammonium bicarbonate (Sigma-Aldrich, St. Louis, MO, USA), pH 8.0] containing 0.1mg/ml trypsin. The peptide mixture, treated with sequencing grade modified trypsin (Promega Biosciences, San Luis Obispo, CA, USA), was concentrated using Zip Tips (Millipore Corp., Billerica, MA, USA).

Peptide samples were mixed at a ratio of 0.5 ml matrix (a-cyano-4-hydroxytranscinnamic acid; Sigma-Aldrich, St. Louis, MO, USA) and 0.5 ml sample, loaded into a 96×2 samples plate (P/N V700813), and crystallized. The crystallized samples were analyzed using an Applied Biosystems Voyager System 4307 MALDI-TOF Mass Spectrometer (Applied Biosystems, Foster City, CA, USA).

Parameters were set as follows: positive ion-reflector mode, accelerating voltage 20 kV, grid voltage 64.5%, mirror voltage ratio 1.12, N_2 laser wavelength 337 nm, pulse width 3 ns, number of laser shots 300, acquisition mass range 800–3500 Da, delay 100 ns, and vacuum degree 4×10^{-7} torr. In addition, des-Arg^1-Bradykinin, Glu^1-Fibrinopeptide B, and ACTH (clip 18-39) were used as external standards for mass calibration.

5. Protein profile distance comparison and clustering analysis

We applied filtering method to the protein expression data to avoid including in the data analysis those proteins that did not vary or that were not highly expressed. We selected only proteins whose expression was significantly different between the normal reference pool and tumor sample pools. The protein spots filtered by student's t-test ($0.05<P$) and

for these spots, we performed protein profile distance comparison and clustering analysis.

The overall distances between protein expression profiles were calculated using the following formula by summing up the absolute ratio of the proteins.

$$\sum_{i=1}^{n} \left| \log_2 \frac{\bar{X}_{ia}}{\bar{X}_{ib}} \right|$$

According to the above-mentioned formula, where n is the number of proteins calculated in the tissue, normalized intensity of protein spots in each a and b sample tissue was used.

The pair-wise distance matrix of protein expression profile was used to build distance trees. The values were entered into a MEGA software program (http://www.megasoftware.net), and the neighbor joining tree was constructed.

Clustering analysis was performed for selected filtered spots. To calculate the protein expression ratios, mean average spot volume of normal reference pools was used for individual normal and tumor samples. The Cluster and Tree View software were used (http://rana.Stanford.EDU/software/) to group proteins with similar expression patterns and to display the tree. We used average linkage clustering with a modified Pearson correlation as similarity metric and protein and array was median centered.

III. RESULTS

1. Clinicopathologic analysis

Clinical information about the ovarian tumor tissues used in this study is shown in table 1. The mean ages of patients with mucinous, endometrioid, and serous tumors were 30.6, 41.3, and 46.5 years, respectively. Mucinous tumors were relatively larger than in the other types, and all were stage I except one endometrioid carcinoma (stage II) and two serous carcinomas (stage II and stage III). Case 1 was taken from two different lesions, one from an adjacent benign cystadenoma (T1a) and another from an intraepithelial carcinoma (T1b). Case 2 ,case 3 and case 5 had no corresponding normal tissues, probably due to the total replacement of ovary by the tumors. Papillary serous carcinomas (PSC) representing with each grade and clinical stage were included in the present study.

Table 1. Clinicopathologic characteristics of tested samples

No.	Age	Histologic type	Mass weight (g) and size (cm)	Stage	Labels tested *
1	25	LMP Mucinous tumor with intraepithelial carcinoma (IEC), non-invasive	1560g/21x16x7cm	I	T1a: cystadenoma T1b: IEC N1: remaining normal tissue
2	32	Microinvasive mucinous ca less than 6mm^2	1230g/25x15x7cm	I	T2: invasive focus
3	28	LMP mucinous tumor, intestinal type	1150g/25x20x8cm	I	T3: IMBT
4	26	LMP mucinous tumor, Mullerian type	540g/8x6x4cm	I	T4: borderline papillae N4: corresponding normal tissue
5	42	Mucinous adenocarcinoma	1550g/8x6x2cm	I	T5: carcinoma
6	35	Endometriotic cyst	25g/6x5x2cm	NS	T6: endometriotic cyst N6: normal tissue
7	49	Endometrioid carcinoma, sertoliform, grade 3/3	533g/12x10x8cm	II	T7: sertoliform N7: corresponding normal
8	40	Endometrioid carcinoma, conventional, grade 1/3	730g/15x13x9cm	I	T8: carcinoma N8: corresponding normal
9	37	LMP serous tumor	45g/7x4x2cm	I	T9: borderline papillae N9: corresponding normal
10	49	Papillary serous ca, grade 1/3	170g/9x5x2.5cm	I	T10: carcinoma N10: corresponding normal
11	50	Papillary serous ca, grade 3/3, with node metastasis	90g/6x4x3cm	III	T11: carcinoma N11: corresponding normal
12	50	Papillary serous ca, grade 3/3, with omental and parametrial invasion	75g/6x4x4cm	II	T12: carcinoma N12: corresponding normal

IEC=intraepithelial carcinoma, LMP= low malignant potential, NS= not stated
IMBT= intestinal mucinous borderline tumor, N: normal, T: tumor
*: labels were nominated according to the areas selected by microdissection

Figure 1 shows the selected areas used for proteomics and microscopic portraits of each tumor. T1 exhibited characteristic stepwise carcinogenesis (intraepithelial carcinoma) directly arising from the conventional IMBT and no definite stromal invasion. Adjacent to the IEC of T1, a benign-looking cystadenoma (T1a) was captured and labeled separately from that of IEC (T1b). T5 exhibited disorderly infiltrative nests with a desmoplastic stroma, whereas T2 showed a small invasive focus less than $10mm^2$, which was compatible with LMP intestinal mucinous tumor with microinvasion. LMP intestinal mucinous tumor (T3) was microscopically similar to a villous adenoma in the gastrointestinal tract, and LMP Mullerian mucinous tumor (T4) showed typical swollen papillae covered by endocervical-like mucinous epithelium. In contrast to a typical endometriotic cyst composed of normal-looking proliferative endometrial glands and stroma (T6), the sertoliform endometrioid carcinoma (T7a) demonstrated cord and trabecular patterns that were less differentiated than a conventional endometrioid carcinoma (T7b).

In comparison with poorly differentiated carcinoma, an extremely well-differentiated endometrioid carcinoma was included (T8). LMP serous tumor (T9) is characterized by detached proliferating papillae with numerous cellular tufts toward the lumen. Three cases of papillary serous carcinomas showed each different clinical stage. Whereas T10 is a well-differentiated PSC encompassing low stage, T11 and T12 are poorly differentiated high stage carcinomas. T11 showed numerous psammomatous calcifications admixed with carcinoma.

A

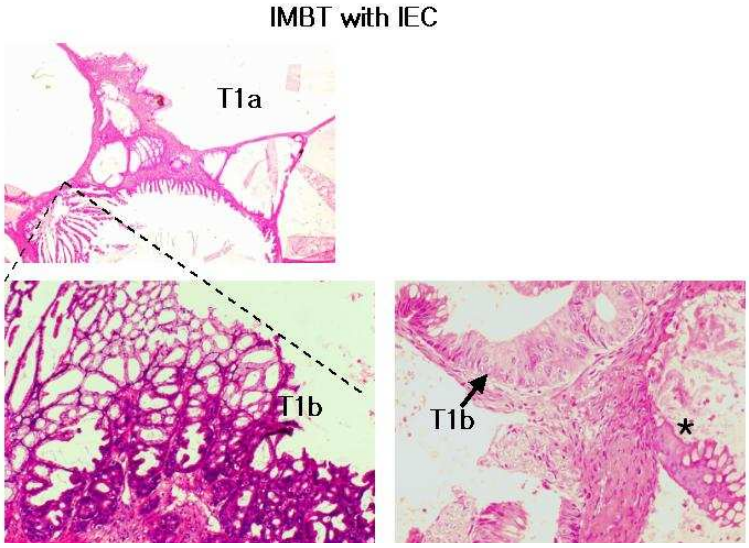
IMBT with IEC
T1a
T1b
T1b
*

B

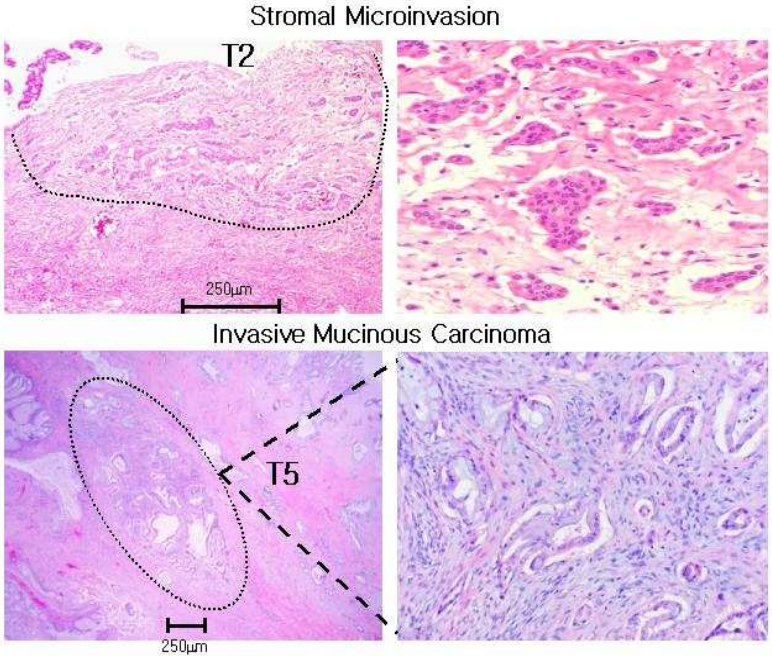
Stromal Microinvasion
T2
250μm
Invasive Mucinous Carcinoma
T5
250μm

C

Intestinal Mucinous Borderline Tumor (T3)

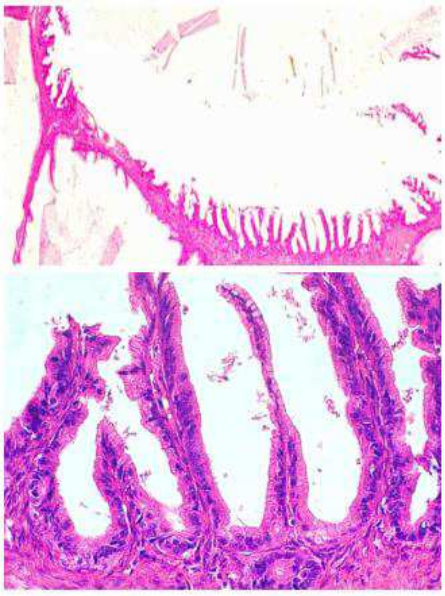

Mullerian Mucinous Borderline Tumor (T4)

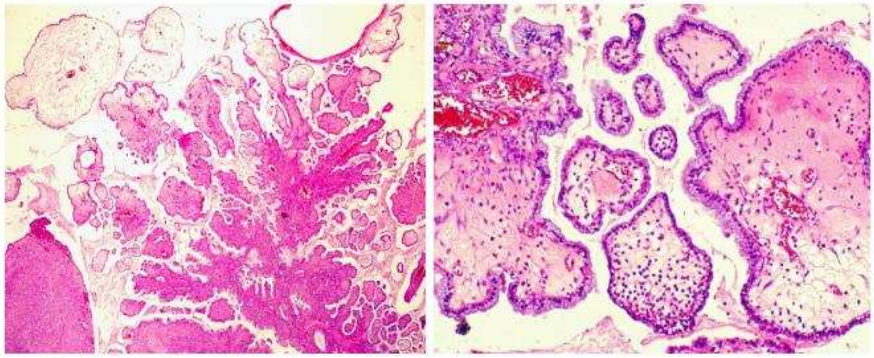

D

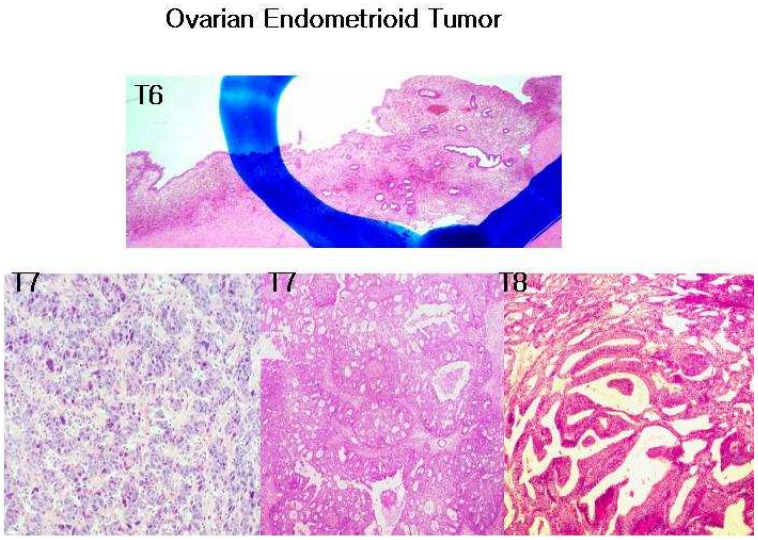
Ovarian Endometrioid Tumor
T6
T7
T7
T8

E

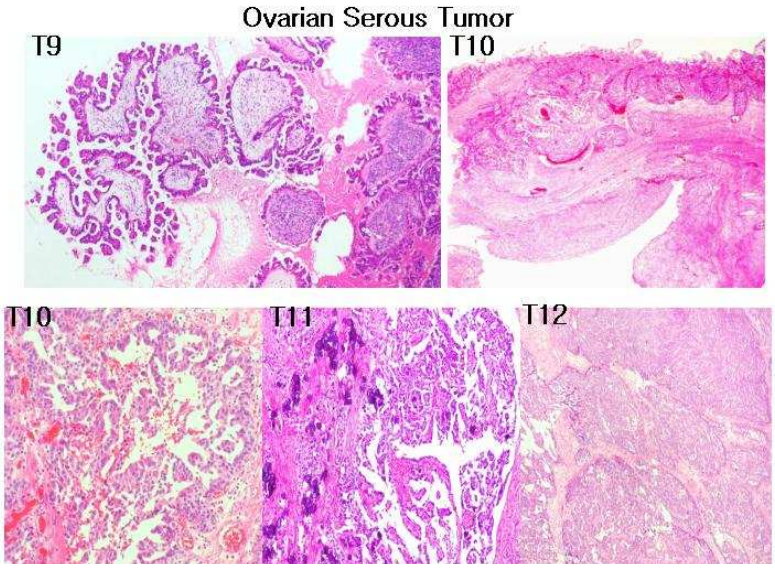
Ovarian Serous Tumor
T9
T10
T10
T11
T12

Fig. 1. Selected areas for proteomics from fresh frozen tissues. A; LMP mucinous tumor with intraepithelial carcinoma. T1 is characteristic of carcinomatous transformation restricted to surface epithelium and no definite stromal invasion arising from the conventional LMP mucinous Mullerian tumor. **B; Ovarian low malignant tumor (LMP).** LMP has two distinct subsets, including LMP mucinous intestinal tumor and LMP mucinous Mullerian tumor. LMP mucinous intestinal tumor (T3) is similar to villous adenoma in gastrointestinal tract, LMP mucinous Mullerian tumor (T4) showed typical swollen papillae covered by endocervical-like epithelium. **C; The stromal invasion in mucinous tumor.** According to the dimension of stromal invasion, LMP mucinous intestinal tumor with microinvasion or invasive carcinoma is determined. Their criteria on the dimension of stromal invasion is $10mm^2$. **D; Endometriotic tumor.** Compare endometriotic cyst with endometrioid carcinoma. Circle area in endometriotic cyst is composed of normal-looking proliferative endometrial glands and stroma (T6). Cord and trabecular pattern appears to be a sertoliform endometrioid carcinoma (T7a) in the more typical endometrioid carcinoma (T7b). Well-differentiated endometrioid carcinoma is identified (T8). **E; Atypical proliferating serous tumor** (T9) is characteristic of detached proliferating papillae with numerous cellular tufts toward lumen. Three cases of papillary serous carcinomas showed each different grade. Well -differentiated PSC (T10) is an early -onset tumor. T11 and T12 demonstrated poorly differentiated carcinomas. T11 showed numerous psammomatous calcifications admixed with carcinoma.

2. Proteomic analysis

A. 2-DE analysis

Proteomic analysis was performed to assess the proteomic similarity or difference of the specific types of epithelial ovarian tumors. For the comparison of LMP tumors, corresponding normal tissues and carcinomas were used as two reference groups (Fig. 2). In the analyzed samples, approximately 1,400 protein spots were detected. In order to analyze similarities or differences in protein expression patterns among the three sample groups, quantity data from 117 spots around a spot without great variation (Fig. 3) were analyzed.

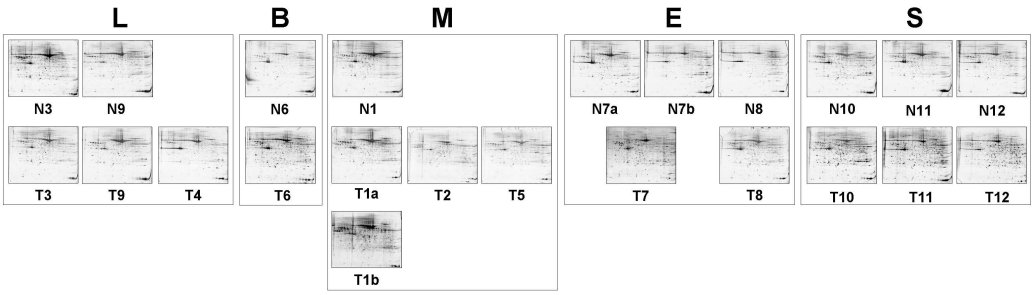

Fig. 2. 2-DE gel images of ovarian cancers and their corresponding normals. For comparing the protein expression differences of the tumor and the paired normal samples, each histologic and biologic different tumor was categorized. **L**; low malignant potential, **B**; benign endometriotic cyst, **M**; mucinous tumor with IEC/invasion, **E**; endometrioid carcinoma, **S**; serous carcinoma, **N**; normal, **T**; tumor

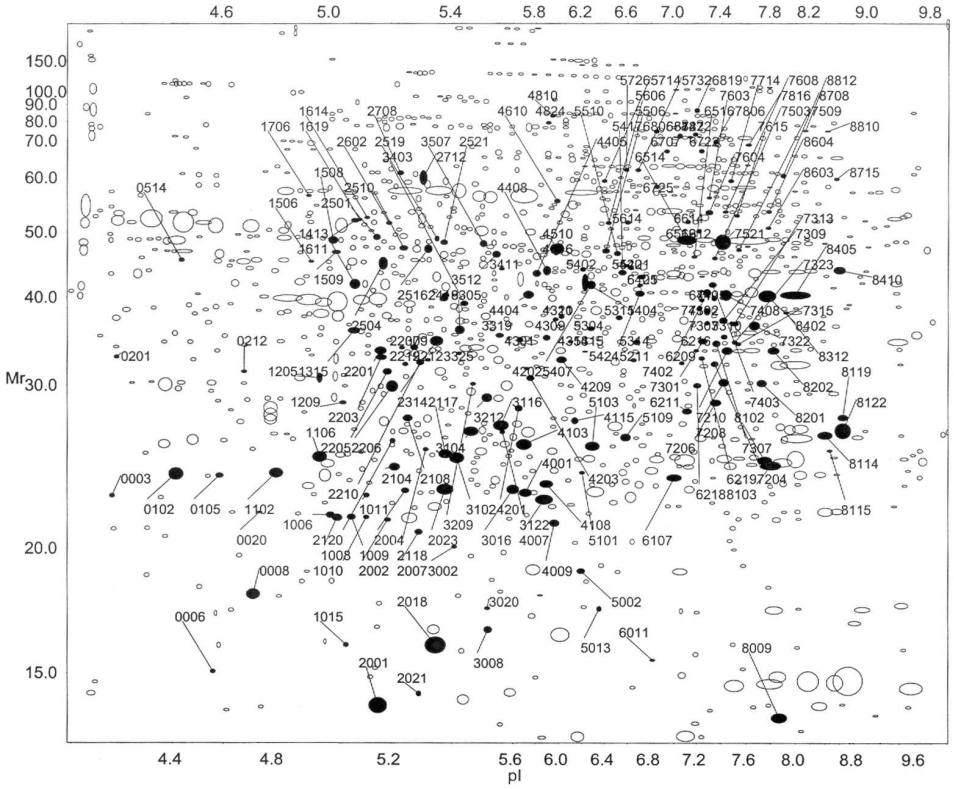

Fig. 3. Nomination of spots on 2-DE.

B. Distance map tree construction

The tree was constructed as a neighbor joining tree by adding the calculated distance of 117 spots as pairwise comparisons and generating a distance matrix. The distance map constructed to assess similarities in the protein expression between samples is shown in Fig. 4A. Group average distance map tree of ovarian epithelial tumors was constructed for estimation of similarities based on Fig. 4A (Fig. 4B). Corresponding normal tissues from the remaining ovarian tissues spared by ovarian tumors aggregated closely to each other. LMP Mullerian mucinous tumor (T4) exhibited an expression pattern quite similar to the normal tissue. LMP intestinal mucinous tumor (T3), LMP serous tumor (T9) and endometriotic cyst (T6) were in the borderline range between the normal and carcinoma groups. LMP tumors with ominous microscopic findings, such as IEC (T1b) or microinvasion less than 10 mm^2 (T2), were separated from the conventional LMP (T3 and T4) and normal group. Even benign-looking cystadenoma areas (T1a) adjacent to the IEC (T1b) showed an identical expression pattern to each other. Invasive mucinous carcinoma (T5) was slightly greater distance from the LMP with IEC or microinvasion. Serous carcinomas (T10, T11, and T12) were found in a cluster at the greatest distance from the normal group, and were apparently different from the mucinous carcinoma. Endometrioid carcinomas (T7 and T8) were between the serous and mucinous carcinomas. Sertoliform endometrioid carcinoma showed a similar map tree to the conventional endometrioid carcinoma.

In terms of serous and endometrioid carcinomas, overall gene expression profiles appeared to be less affected by grading or stage,

than by histologic type.

The degree of similarity or difference between three distinct ovarian epithelial carcinomas was analyzed by the relative extent of expression ratio when we use the initially branched point (asterisk in Fig. 4A) as a reference.

When type-specific differences were compared, mucinous carcinoma was different from the papillary serous carcinoma or endometrioid carcinoma by 1.98-fold. The ratio of endometrioid carcinoma to serous carcinomas was 1.1-fold, both of them represent similar to each other (Fig. 4C).

A

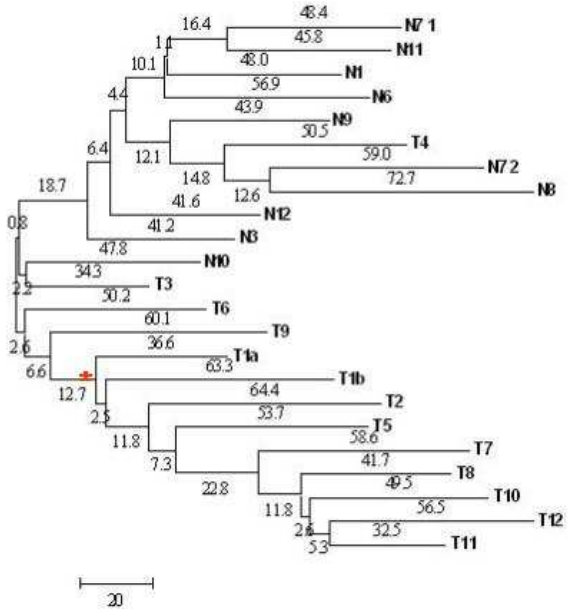
16.4
48.4
N7 1
45.8
N11
48.0
10.1
N1
56.9
4.4
N6
43.9
N9
50.5
6.4
12.1
T4
59.0
N7 2
14.8
72.7
18.7
12.6
N8
41.6
N12
0.8
41.2
N3
47.8
N10
34.3
T3
2.2
50.2
T6
60.1
T9
2.6
36.6
T1a
6.6
63.3
T1b
12.7
64.4
T2
2.5
53.7
T5
11.8
58.6
T7
7.3
41.7
T8
22.8
49.5
T10
11.8
56.5
T12
2.6
32.5
5.3
T11
20

B

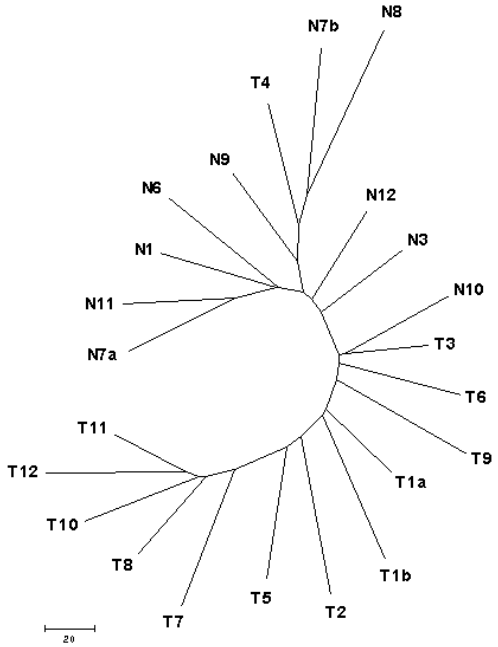
N8
N7b
T4
N9
N6
N12
N3
N1
N10
N11
T3
N7a
T6
T11
T9
T12
T1a
T10
T1b
T8
T5
T2
T7
20

C

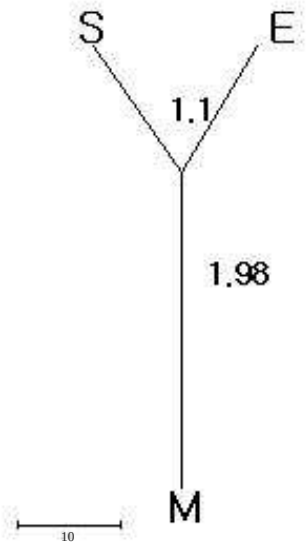

Fig. 4. Map tree of ovarian epithelial tumors.

S=serous, **M**=mucinous, **E**=endometrioid

A; Clustering of distance map tree. Numbers refer to the ratio between the changes common to ovarian epithelial tumors. Each tumor is categorized according to protein expression extents.

B; Distance tree representing the relative extents of expression changes between ovarian tumors and corresponding normal tissues.

C; Group average distance map tree of ovarian epithelial tumors. This represents the relative extend of expression difference between three different ovarian carcinomas when serous carcinoma group is a reference.

C. Clustering algorithm of ovarian tumors

In previous distance analysis of protein expression profile, we showed that protein expression profile discriminate the features of tumor type classified by histologic observation. Although profile distance analysis reflected relative distances of similarities or differences of expression profiles, these calculations neglected the orientation of expression pattern. For example, simultaneously two fold up-regulated or down-regulated pattern showed same distance.

In this reason, hierarchical clustering analysis was performed to compare the similarity according to expression patterns. All 117 spots applied to the previous profile distance analysis were also adopted for clustering analysis.

As shown in Fig. 5 thirteen tumor samples were classified principally into three groups. The expression profiles of the serous carcinomas were isolated forming sub-class consisting two endometrioid carcinomas in one group. Five mucinous tumors were clustered in one group. In previous profile distance analysis, T4 mucinous tumor was separated from the rest of mucinous tumors showing rather similar expression profile to the normal tissue. Interestingly, in this cluster analysis, T4 was represented similar pattern to the mucinous tumor although T4 formed subclusters with T5. In the clustergram comprised overall normal and tumor samples, T4 also showed more similar pattern to normal than the rest of the mucinous tumors.

This fact implied that T4 did not reveal distinct expression profile to the mucinous tumors, however, T4 shared more common expression pattern with mucinous tumors rather than other types of tumors.

The last group consisting of two borderline tumors was isolated from the two principal groups. In this analysis, distinct three groups were classified from protein expression profile, although the distance relationship was not clearly deciphered.

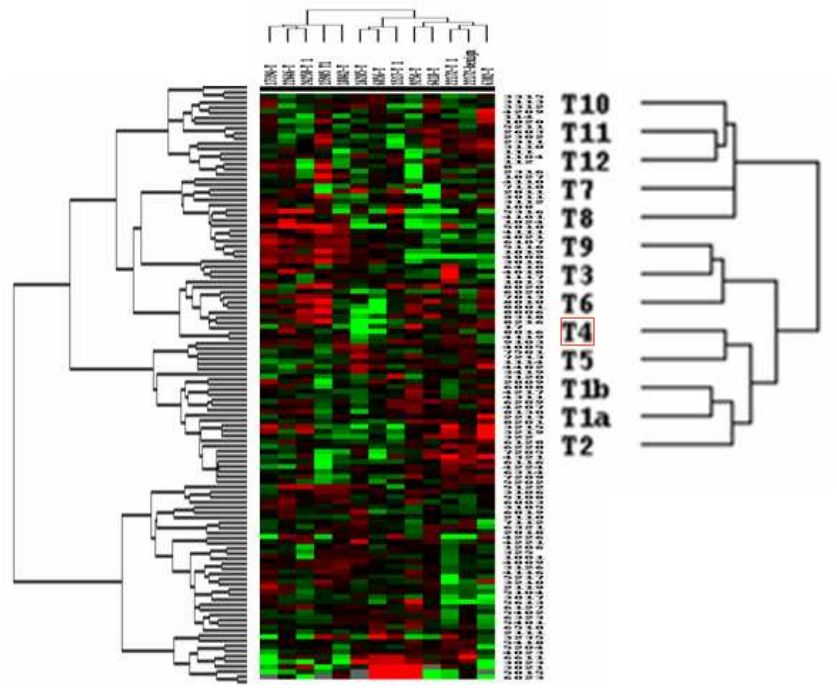

Fig. 5. Clustergram of ovarian tumor expression profile. Left panel represents the expression pattern of thirteen tumor expression profile. This clustergram was constructed from differentially expressed 117 spots as compared with normal groups. **Right panel** represents the dendrogram showing the similarity relationship of thirteen tumors. In scale bar, green color represents the fold of down-regulation, and red represents the fold of up-regulation of protein expression.

IV. DISCUSSION

A distance tree based on intra- and inter-tumoral variations of gene expression patterns was first adopted to determine similarities between several organs from different species of primates.[14] The present study, which aimed to phylogenetically classify and determine proteomic similarities between epithelial ovarian tumors, is the first application of distance map tree proteomics in human tumors. In particular, we focused on the evaluation of mucinous tumors, between conventional LMP and LMP with histologic ominous features, such as IEC or microinvasion. This was feasible due to the quantitative differences in protein expression profiles between closely related epithelial tumors. It is likely that there are numerous underlying reasons for such expression differences, for instance: duplications and deletions of genes, promoter changes, changes in levels of transcriptional factors, and changes in cellular compositions of tissues.[14,15]

In general, mucinous tumors have been known to be more prevalent among younger patients and are more frequently associated with borderline or benign spectrums than serous or endometrioid tumors.[6,8] Therefore, some mucinous tumors are thought to develop through stepwise genetic alterations, in contrast to serous carcinomas, which are thought to arise de novo from the ovarian surface epithelium and its inclusion cysts.[6,8,16] We recognized that ovarian mucinous tumors are apparently distinct from other ovarian surface epithelium-derived epithelial tumors in their protein expression profiles.

Interestingly, we observed that morphologic heterogeneity in

mucinous tumors does not result in proteomic heterogeneity, which was demonstrated by the divergent morphologic areas in the same mucinous tumor having similar proteomic alterations.

The first evidence of this is that the protein expression profiles of benign cystadenoma were more likely to those of adjacent intraepithelial carcinoma than those from the corresponding normal areas. The second evidence is that the phylogenetic tree of LMP mucinous tumors with microinvasion was very close to that of widely invasive mucinous carcinoma. All LMP tumors showing histologic ominous features, such as LMP mucinous tumors with IEC or microinvasion, were distinctively different from LMP mucinous tumors and took protein expression patterns of mucinous carcinoma in overall protein expression profiles.

Mucinous intraepithelial carcinomas have been defined conceptually same as carcinoma in situ, and foci of stromal invasions <10mm^2 have been designated “LMP with microinvasion” since cases with such findings have had more favorable outcomes than mucinous carcinoma in previous studies.[8,17,18] However, their biological behaviors remain unknown, not only because of a lack of discernable protein profiles between LMP and IEC or microinvasive tumors, but also because there have been very few studies on these tumors.

We speculate that ovarian mucinous tumors may take the proteomic portraits from their worst histological features, based on the results in the present study exhibiting the same protein profiles even in benign or borderline areas adjacent to the carcinoma. This scenario is consistent with the previous study for detection of the same genetic aberrance, i.e.

k-ras mutation, in separate areas exhibiting different histologic grades within the same mucinous tumor.[16] Nonetheless, the protein expression profiles of Mullerian LMP mucinous tumors are nearly the same as normal tissue, which may explain why they are not fatal and have excellent clinical behavior.[19,20]

In the phylogenetic map tree, serous carcinomas were obviously separated from mucinous carcinomas. Serous carcinomas were located the greatest distance from the normal and LMP groups, whereas mucinous carcinomas were more close to the normal group. This protein expression profile of serous carcinomas may explain their highly aggressive clinical behavior of this tumor.

As expected, high stage serous carcinomas (T11 and T12) were slightly separated from the stage 1 serous carcinoma (T10). Endometrioid carcinomas were mapped between the serous and mucinous carcinomas. Sertoliform endometrioid carcinoma, a variant of poorly differentiated endometrioid carcinoma, was found to be of a common lineage with conventional endometrioid carcinoma at least in overall protein expression profiles.

When we compared type-specific differences, we found that the change of mucinous carcinomas was 1.98-fold that of serous carcinomas, and the ratio of endometrioid carcinoma to serous carcinomas was 1.1-fold. These results show that mucinous carcinomas are different from serous and endometrioid carcinomas, which may reflect the improved prognosis of mucinous carcinomas.

V. CONCLUSION

In the present study, we identified that ovarian malignant epithelial tumors showed distinctively different protein expression profiles between histological subtypes. Serous carcinoma was the most different from the normal group, while mucinous carcinoma was the least different. LMP mucinous tumors with IEC and stromal microinvasion exhibited the molecular expression pattern closer to mucinous carcinoma rather than LMP mucinous tumors, which means that LMP mucinous tumors showing histologic aggressive features belong to mucinous carcinoma on the proteomic basis. Furthermore, the morphologic continuous spectrum in mucinous carcinoma has the same protein expression profiles.

REFERENCES

1. Auersperg N, Wong AST, Choi K, Kang S, Leung PCK. Ovarian surface epithelium: biology, endocrinology, and pathology. Endocr Rev 2001; 22:255-288.
2. Auersperg N, Pan J, Todd P, Fischer J, Somasiri A, Grove BD, et al. E-cadherin induces mesenchymal-to-epithelial transition in human ovarian surface epithelium. Proc Natl Acad Sci USA 1999; 96:6249-6254.
3. Ong A, Maines-Bandiera S, Roskelley CD, Auersperg N. An ovarian adenocarcinoma line derived from SV40/E-cadherin transfected normal human ovarian surface epithelium. Int J Cancer 2000; 85:430-437.
4. Link CJ, Kohn E, Reed E. The relationship between borderline ovarian tumors and epithelial ovarian carcinoma: epidemiologic, pathologic and molecular aspects. Gynecol Oncol 1996; 60:347-354.
5. Shih I, Kurman RJ. Ovarian tumorigenesis. A proposed model based on morphological and molecular genetic analysis. Am J Pathol 2004; 164:1511-1518.
6. Lee KR, Tavassoli FA, Prat J. Surface epithelial-stromal tumors. In: Tavassoli FA and Deville P, Editors. WHO Classification of Tumors. Tumors of the breasts and female genital organs. Lyon:IARC Press; 2003. P.117-145.
7. Powell DE, Puls LE, Nagell JR. Current concepts in epithelial ovarian tumors: does benign to malignant transformation occur? Hum Pathol 1992; 23:846-847.

8. Rodriguez IM, Prat J. Mucinous tumors of the ovary: a clinicopathologic analysis of 75 borderline tumors (of intestinal type) and carcinomas. Am J Surg Pathol 2002; 26:139-152.
9. Wulfkuhle JD, Aquino JA, Fishman Da, Coukos G, Liotta LA, Calvert VS, et al. Signal pathway profiling of ovarian cancer from human tissue specimens using reverse-phase protein microarrays. Proteomics 2003; 3:2085-2090.
10. Jones MB, Krutzsch H, Zhang Y, Liotta LA, Kohn EC, Shu H, et al. Proteomic analysis and identification of new biomarkers and therapeutic targets for invasive ovarian cancer. Proteomics 2002; 2:76-84.
11. Alexe G, Alexe S, Hammer BL, Petricoin E, Reiss M, Liotta LA, et al. Ovarian cancer detection by logical analysis of proteomic data. Proteomics 2004; 4:766-783.
12. Conrads TP, Johann D, Steinberg SM, Kohn EC, Fusaro VA, Ross S, et al. High-resolution serum proteomics features for ovarian cancer detection. Endocrine-related Cancer 2004; 11:163-178.
13. Nicosia SV, Bai W, Cheng JQ, Coppola D, Kruk PA. Oncogenic pathways implicated in ovarian epithelial cancer. Hematol Oncol Clin North Am 2003; 17:927-943.
14. Enard W, Khaitovich P, Zollinger S, Heissig F, Giavalisco P, Klose J, et al. Intra- and interspecific variation in primate gene expression patterns. Science 2002; 296:340-346.
15. Saitou N, Nei M. The neighbor-joining methods: a new method for reconstructing phylogenetic trees. Mol Biol Evol 1987; 4:406-425.

16. Cuatrecasas M, Villanueva A, Matias-Guiu X, Prat J. K-ras mutations in mucinous ovarian tumors. A clinicopathologic and molecular study of 95 cases. Cancer 1997; 79:1581-1586.
17. Lee K, Scully RE. Mucinous tumors of the ovary. A clinicopathologic study of 196 borderline tumors (of intestinal type) and carcinomas, including an evaluation of 11 cases with 'pseudomyxoma peritonei'. Am J Surg Pathol 2000; 24:1447-1464.
18. Shappell HW, Riopel MA, Ronmett BM, Kurman RJ, Sehdev AE. Diagnostic criteria and behavior of ovarian seromucinous tumors. Atypical proliferative (borderline) tumors, intraepithelial, microinvasive and invasive carcinoma. Am J Surg Pathol 2002; 26:1529-1541.
19. Siriaounkgul S, Robbins KM, McGowan L, Silverberg SG. Ovarian mucinous tumors of low malignant potential: a clinicopathologic study of 54 tumors of intestinal and Mullerian type. Int J Gynecol Pathol 1995; 14:198-208.
20. Nomura K, Aizawa S. Clinicopathologic and mucin histochemical analysis of 90 cases of ovarian mucinous borderline tumors of intestinal and Mullerian types. Pathol Int 1996; 46:575-580.

Abstract (in Korean)

비교 단백체를 이용한 상피성 난소종양의 재분류

<지도교수 **김 세 광**>

연세대학교 대학원 의학과

박 용 규

난소종양은 인체에 발생하는 종양 중 가장 다양한 조직학적 유형을 보이는 종양 중의 하나이며 일반적인 종양의 개념과는 생물학적 양상이 많이 다르다. 이러한 예외적인 생물학적 양상 때문에 명칭이나 기전, 그리고 정확한 진단이 용이하지 않으며 이로 인해 병리적인 개념이 정확해야 알아낼 수 있는 분자 생물학적 이해 또한 정확히 알려진 사실이 많지 않다.

최근 들어 개별적인 유전자 연구가 아닌 high throughput technique이 발달하면서 RNA단계에서는 c-DNA array, 단백 단계에서는 proteomics 연구가 활발히 진행되고 있는데, 이들 모두 신선한 냉동조직이 필수로 확보되어야 하며, 또한 종양부위를 정확히 확인할 수 있는 병리적 개념을 갖춘 경험 있는 연구자가 시행한 경우에 가장 이상적인 연구결과를 얻을 수 있다.

그러나 난소종양은 다른 종양과는 달리 분자병리 영역의 연구를 하기 위해 필요한 신선한 조직을 확보하는데 상당한 어려움이 따른다. 즉 육안소견으로 진단을 추정할 수 있는 경우가 많지 않을 뿐 아니라, 낭성종

양인 경우, 적절한 부위를 선택하기에 어려움이 많다. 또한 괴사와 출혈이 유난히 많기 때문에 병리학적으로 충분한 경험이 있어야만 정확한 부위를 선택할 수 있다. 더구나 같은 종양이라도 조직학적 유형과 종양의 성격이 매우 다양하므로 올바른 종양의 분류실험이 용이하지 않다.

이상과 같은 이유 등으로 대부분의 난소종양의 분자병리영역의 연구는 그 동안은 주로 세포주에 관련된 연구가 대부분이며, 인체조직내의 난소종양의 연구는 매우 미미한 수준으로 대부분 형태학적 면역화학적 실험에 그치고 마는 것이 현실이었다.

본 연구는 병리학적으로 정확하게 종양부위를 확인하고 수집된 12예의 신선한 난소종양 조직을 확보하여, 확보된 부위를 병리학적으로 재검색한 후 종양부위를 병리학적으로 표시하여 laser capture를 이용한 미세박절을 시행하여 얻은 단백질을 이용하여 난소종양의 단백체 차이를 비교함으로써 protein profiling을 구축하였다. 2-D gel에서 비교하여 2배 이상의 차이를 보이는 단백질들의 발현강도를 합산하여 비교치와의 비율로 거리값으로 환산하여 Cluster and Tree View software를 이용하여 표현하였다

12예의 난소종양은 4예의 장액성 종양, 5예의 점액성 종양, 3예의 자궁내막양 종양이었으며, 4예의 장액성 종양 중 1예는 경계성 종양이었고, 5예의 점액성 종양 중 2예는 경계성 종양이었다. 3예의 점액성 악성종양은 병리학적으로 1예는 상피내 악성화가 진행된 경우이었고, 다른 1예는 간질조직내로 $10mm^2$ 이내로 침윤한 미세침윤형 점액성 종양이었으며 나머지 1예는 $10mm^2$ 이상 침윤을 보인 악성 종양이었다. 특히 상피내 악성화를 보인 1예는 주변의 양성 낭성 종양 부위도 별도로 검색하였다.

본 연구에서는 다른 분화를 보이는 종양이나 경계성 영역 등의 애매한 예후를 보이는 종양의 해석에 도움을 줄 것으로 생각하여 비교 대상군간에 나타나는 단백체 발현군 중 의미 있게 차이를 보이는 부분을 전체 합산하여 비교함으로써 대조군에서 비교군이 어느 정도 위치하는지를 계

통적으로 map tree를 구성하여 분석하였다. 여러 난소종양 중 점액성 경계성 종양은 정상군과 같은 거리에 위치하며, 점액성 상피내 암종이나 미세침윤성 종양과 같이 악성으로 분류되지만 경계성 종양의 예후를 보이는 것으로 알려진 종양은 단백체 map tree 결과만으로는 확실히 경계성 점액성 종양과는 다른 군에 속함으로써 단백체적으로 다른 종양임을 시사하였다.

또한 점액성 종양은 흔히 악성과 함께 경계성 혹은 양성 낭성조직이 동시에 관찰되는 경우가 많은데, 한 종양내 형태학적으로 상이한 부위, 즉 상피내 악성종양을 보이는 곳과 양성낭성처럼 보이는 부위의 상호비교 결과 동일한 위치에 속함을 알 수 있어, 형태학적인 차이가 달라도 한 종양내 분자생물학적인 차이는 같음을 알 수 있었다.

점액성 암종에서 관찰된 침윤성 부위와 경계성 혹은 양성조직이 모두 같은 단백체적 양상을 보이며 이는 분명히 경계성 종양과는 다른 소견을 본 연구결과에서 확인할 수 있었다. 장액성 암종은 정상군과 가장 거리가 먼 위치에 속하며 자궁내막양 암종과는 매우 근접함을 보인 반면 점액성 종양과는 약 1.98배의 거리 비율을 보여 map tree 결과로 보면 장액성과 점액성 종양은 상이한 종양임을 알 수 있었다.

결론적으로 상피성 난소종양을 대상으로 단백체를 비교분석한 결과 점액성 암종에서 관찰된 침윤성 부위와 경계성 혹은 양성조직이 모두 같은 분자 유전학적 양상을 보이며 이는 분명히 경계성 종양과는 다른 소견을 본 연구결과에서 확인할 수 있었을 뿐 아니라, 점액성 종양은 다른 상피기원 종양인 장액성 및 자궁내막양 종양과는 단백체 발현상 의미있는 차이를 보였다.

핵심되는 말 : 상피성 난소종양, proteomics, distance map tree, low malignant potential